Molecular Origin of the Anomalous Thermodynamic Behavior of Single-site Ethylene-1-octene Copolymer Liquids with Different Branch Contents

Z. H. Liu, M. Zhang, L. Zhao, and P. Choi*

Department of Chemical and Materials Engineering, University of Alberta, Edmonton, Alberta, Canada T6G 2G6

Received January 28, 2005; Revised Manuscript Received March 3, 2005

ABSTRACT: Zero-pressure-weight-fraction Henry's constants (H_{12}^0) and infinite-dilution-weight-fraction activity coefficients (Ω_1^∞) of selected aliphatic and aromatic solvents in a series of single-site ethylene-1-octene copolymers (ss-EOs) with different branch contents were measured using inverse gas chromatography over the temperature range from 170 to 230 °C. It was observed that measured H_{12}^0 of solvents with high volatility exhibited a minimum in the branch content range of 0−20 branches per 1000 backbone carbons but were independent of branch content over the range from 20 to 87, while that of solvents with low volatility was insensitive to branch content at all. The observed behavior became more pronounced for highly volatile solvents and propagated to solvents with medium volatility as temperature was increased. It was found that the observed minima are mainly attributed to the relatively more favorable interactions between the solvents and the copolymers with branch contents less than 20, as quantified by the measured Ω_1^∞. However, for the solvents with extremely low volatility, such favorable changes in Ω_1^∞ in the low branch content region did not manifest themselves in the measured H_{12}^0 as these changes were completely masked by the low volatility of the solvents even at 230 °C. Molecular dynamics (MD) simulation results on comparable ss-EO models with branch contents from 0 to 90 suggested that the observed Ω_1^∞ behavior may originate from changes in the free volume hole size distribution, not from changes in the specific free volume of the copolymer. In particular, the simulation results showed that regardless of the temperature, the volume fraction of spherical free volume holes with radii larger than 1.5 Å decreased as the branch content was increased, while the specific free volume stayed constant.

Introduction

It has long been recognized that single-site ethylene-1-octene copolymer (ss-EO) possesses a higher degree of intermolecular branch content homogeneity than EO synthesized with the use of Ziegler−Natta catalysts (ZN-EO). It is generally believed that such a difference leads to the observed differences in a variety of mechanical properties of the two types of copolymers. For example, ZN-EO shows a higher tear resistance but a lower dart impact resistance than ss-EO.[1] Most recently, using the technique of inverse gas chromatography (IGC), we have demonstrated that the two types of copolymers with comparable molecular characteristics (e.g., molecular weight averages, average branch content (i.e., number of branches per 1000 backbone carbons), etc.) in their liquid state exhibit very different abilities to absorb hydrocarbon solvents at elevated temperatures.[2] This was somewhat surprising, considering the fact that both polymers possess similar chemical structures and that they are in their amorphous state at high temperatures. In particular, at a fixed temperature and for a given hydrocarbon solvent, our previous work showed that zero-pressure-weight-fraction Henry's constants (H_{12}^0) of ss-EO exhibit a slightly increasing trend with increasing branch content over the range from 10 to 35 while that of ZN-EO decreases significantly. Since H_{12}^0 is mainly determined by the volatility of the solvent and its interaction with the polymer in the liquid state at a fixed temperature[3], the observation simply suggests that the two polymers may have very different liquid morphology (i.e., local packing patterns of the molecules). To confirm such a speculation, we extended our IGC study to a series of ss-EOs covering a wider range of branch contents from 0 (i.e., high-density polyethylene (HDPE)) to 87. We also carried out molecular dynamics (MD) simulations on comparable model ss-EO molecules to discern the effect of branch content on the copolymer's liquid morphology. It should be noted that it would be most desirable to include ZN-EOs with a similar range of branch contents in the study. However, such samples were not available.

* Author to whom correspondence should be addressed. Email: phillip.choi@ualberta.ca.

Experimental Section

Materials. One HDPE and five ss-EOs with different average branch contents were used in the present work. The HDPE and the low branch content ss-EOs were supplied by NOVA Chemicals Corporation, while the two highest branch content ss-EOs were obtained from ExxonMobil Chemicals Corporation. Table 1 summarizes some of their physical characteristics, as provided by their respective manufacturers.

Twelve reagent grade solvents, purchased from Fisher Scientific Company, were used in the IGC measurements. They consisted of saturated linear aliphatic hydrocarbons (*n*-hexane, *n*-heptane, octane, *n*-nonane, *n*-dodecane, and *n*-pentadecane), unsaturated aliphatic (1-hexene and 1-octene), saturated circular aliphatic (cyclohexane), and aromatic (benzene, toluene, and xylenes). They were used as received without further purification. Their molecular formulas, normal boiling points, and van der Waals volumes, obtained from refs 4 and 5, are depicted in Table 2.

Column Preparation and Measurements. A total of six IGC packed columns were prepared. Standard IGC packed column preparation and column conditioning procedures were followed.[6] The mass of the polymer packed into each IGC column was determined by a calcination method with blank corrections. The characteristics of all columns are shown in Table 3. Net retention times of the above-mentioned solvents

10.1021/ma0501904 CCC: $30.25
Published on Web 04/06/2005

Table 1. Densities, Molecular Weight Averages, and Average Branch Contents of the HDPE and ss-EOs Used in the Present Work

polymer	manufacturer	density at 25 °C (g/cm^3)	molecular weight averages M_n	M_w	branch content (number of branches per 1000 carbons)
HDPE	NOVA	0.962	13700	49400	~0
ss-EO-1	NOVA	0.938	34600	69200	3
ss-EO-2	NOVA	0.922	38700	77400	11.4
ss-EO-3	NOVA	0.914	20300	69000	18.1
ss-EO-4	ExxonMobil	0.874	53800	96900	49.7
ss-EO-5	ExxonMobil	0.865	52000	104000	87.2

Table 2. Molecular Formulas, van der Waals Volumes, and Normal Boiling Points of the 12 Hydrocarbons Used in the Present Work

hydrocarbon	molecular formula	van der Waals volume Å^3/molecule[a]	normal boiling point (°C)
1-hexene	C_6H_{12}	109.72[b]	60−66
n-hexane	C_6H_{14}	112.24	69
benzene	C_6H_6	95.9	80
cyclohexane	C_6H_{12}	103.8	80.7
n-heptane	C_7H_{16}	129.53	98
toluene	C_7H_8	113.2	110−111
1-octene	C_8H_{16}	114.32[b]	122−123
octane	C_8H_{18}	146.81	125−127
xylenes	C_8H_{10}	115.78[b]	137−140
n-nonane	C_9H_{20}	164.09	151
n-dodecane	$C_{12}H_{26}$	215.94	215−217
n-pentadecane	$C_{15}H_{32}$	267.78	270

[a] Data were taken directly from ref 5. [b] Data were calculated using eq 4 in ref 5.

were measured for all columns at four temperatures (170, 190, 210, and 230 °C). The corresponding specific retention volumes (V_g^0) were then calculated using eq 1 in which the net retention times (t_R) were corrected by subtracting the retention time of the marker (i.e., methane) (see eq 2).

$$V_g^0 = \frac{273.15 t_R F J}{w T} \tag{1}$$

$$t_R = t_{\text{solvent}} - \left(t_{CH_4} - \frac{w T R}{H^0_{CH_4} F J} \right) \tag{2}$$

In the above equations, F is the carrier gas flow rate, J is the James−Martin correction factor, which is determined by the inlet and outlet pressures of an IGC column, w is the mass of the polymer that is packed into the column, T is the experimental temperature, and R is the universal gas constant.

Zero-pressure-weight-fraction Henry's Constant (H_{12}^0) and Infinite-dilution-weight-fraction Activity Coefficient (Ω_1^∞). Once the specific retention volume is obtained, zero-pressure-weight-fraction Henry's constant (H_{12}^0) and infinite-dilution-weight-fraction activity coefficients (Ω_1^∞) can then be calculated using eqs 3 and 4, respectively. The derivations of the equations and the assumptions involved in the derivations are described elsewhere.[7, 8]

$$H_{12}^0 = \left(\frac{273.15 R}{V_g^0 M_1} \right) \tag{3}$$

$$\ln \Omega_1^\infty = \ln\left(\frac{273.15 R}{P_1^0 V_g^0 M_1} \right) - \frac{P_1^0 (B_{11} - V_1)}{RT} \tag{4}$$

Here, M_1 is the molecular weight of the solvent, P_1^0 is its

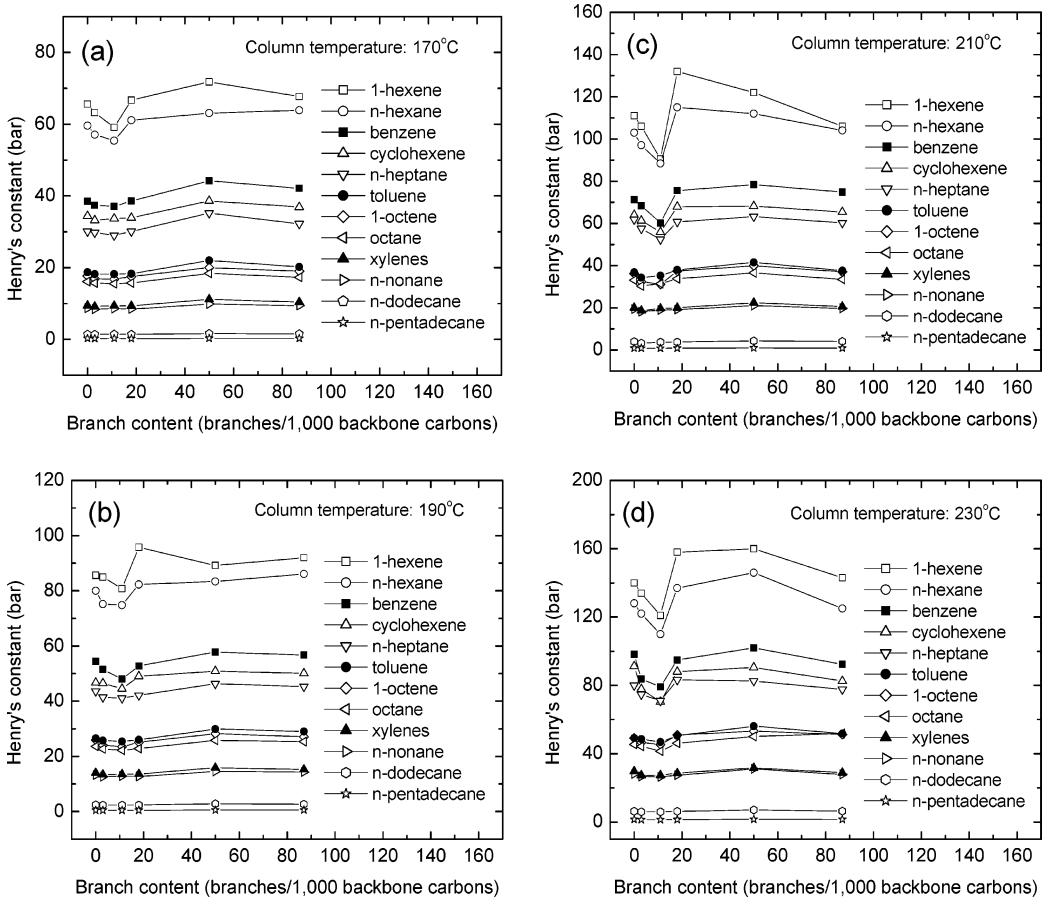

Figure 1. Branch content dependence of zero-pressure-weight-fraction Henry's constant at four elevated temperatures (a) 170, (b) 190, (c) 210, and (d) 230 °C, respectively, for all 12 hydrocarbon solvents used.

Table 3. Operating Conditions of the IGC Columns Packed with Pure HDPE and Five ss-EOs

	HDPE	ss-EO-1	ss-EO-2	ss-EO-3	ss-EO-4	ss-EO-5
mass coated (g)	0.05396	0.04920	0.04920	0.04920	0.04920	0.04920
loading (%)	8.80	7.14	7.14	7.14	7.14	7.14
solid support	Chromosorb W, DMCS treated and acid washed, mesh size: 60/80					
column length (m)	1					
column OD (m)	6.35×10^{-3}					
inlet pressure (kPa)	200−250					
outlet pressure (kPa)	95−105					
carrier gas	purified helium					
flow rate (mL/min)	23−25 depending on the temperature					

Table 4. Energy Expressions and the Associated Force Field Parameters Used in the Drieding 2.21 Force Field

		parameter	
interaction	expression		
bond energy	$E_b = \frac{1}{2}K_b(R - R_0)^2$	$K_b = 2.93 \times 10^5$ kJ/mol/nm^2	
		$R_0 = 0.15$ nm	
angle energy	$E_\theta = \frac{1}{2}K_\theta(R - R_\theta)^2$	$K_\theta = 418$ kJ/mol/rad^2	
		$R_\theta = 1.91$ rad	
torsion energy	$E_\phi = \sum_{n=1}^{2} \frac{1}{2}K_{\phi,n}[1 \pm \cos(n\phi)]$	$K_\phi = 20.9$ kJ/mol	
inversion energy	$E_{\text{inv}} = K_{\text{inv}}(\cos\chi - \cos\chi_0)^2$	$K_{\text{inv}} = 20.9$ kJ/mol	
		$\chi_0 = 2.09$ rad	
van der Waals energy	$E_{\text{vdw}} = \epsilon_0\left[\left(\frac{\sigma_0}{R}\right)^{12} - 2\left(\frac{\sigma_0}{R}\right)^6\right]$	C with one implicit H	$\epsilon_0 = 0.6985$ kJ/mol
			$\sigma_0 = 0.3923$ nm
		C with two implicit H	$\epsilon_0 = 0.6985$ kJ/mol
			$\sigma_0 = 0.3923$ nm
		C with three implicit H	$\epsilon_0 = 0.6985$ kJ/mol
			$\sigma_0 = 0.3923$ nm
		off-diagonal interactions	geometric mean was used for ϵ_0, while arithmetic mean was used for σ_0

vapor pressure, and B_{11} and V_1 are the second virial coefficient and liquid molecular volume of the solvent, respectively, at the experimental temperature T. Note that for a given solvent at a fixed T, P_1^0, B_{11}, and V_1 are all known quantities that were obtained from standard sources on thermophysical properties of the solvents used such as refs 4 and 9.

Molecular Modeling

To discern the effect of branch content on the local packing patterns of the ss-EOs of interest, MD simulations were carried out using one HDPE and four ss-EO single-chain united-atom models. The branch contents of the models used were 0, 10, 20, 50, and 90. For each model, the hexyl branches were randomly distributed along the backbone of the model molecule that contained 1000 united carbon atoms. A generic force field, Drieding 2.21,[10] was used to describe the intra- and intermolecular interactions. The corresponding energy expressions and the associated force field parameters are shown in Table 4. Use of Drieding 2.21 was based upon our previous experience that the force field yields fairly accurate results on solubility parameters of polyethylene at elevated temperatures using a canonical (i.e., NVT) ensemble along with the available experimental density.[11−13] Nose canonical method with a Leapfog numerical algorithm was used at two simulation temperatures, 425 K (152 °C) and 525 K (252 °C) over a simulation time period of 1000 picoseconds (i.e., 1 ns) with a time step of 1 fs.[14] All MD simulations were implemented on a SGI workstation cluster using the software Cerius^2 version 4.6 from Acceryls.

In general, the morphology (i.e., local packing patterns) of molecules in the liquid state can be described either by their intermolecular pair correlation functions (PCFs) or backbone carbon−carbon bond trans/gauche (t/g) ratios. However, in the present work, we calculated the size distribution of the free volume holes instead as it is a more convenient variable to be used to interpret our IGC data. Nevertheless, the size distribution of the free volume holes should be intimately related to the packing patterns of the molecules. Because the specific free volume of a polymer (i.e., the total free volume per unit mass of the polymer) contains free volume holes with different sizes and shapes, the computed specific free volume naturally depends on the size of the probe, usually in the spherical shape, used. As one can imagine, an extremely large probe would give zero free volume as such a probe could not be inserted into the model bulk material. However, we utilized such probe size dependence of specific free volume to determine the volume fractions (i.e., size distribution) of the free volume holes with different sizes. This was simply accomplished by computing the specific free volumes of each model using a series of spherical probes with radii over the range from 0.6 to 3.0 Å, allowable by Cerius^2, with an increment of 0.1 Å. Obviously, the difference between the free volumes detected by two probes with adjacent sizes equal the free volume detected by the smaller one. Addition of all such free volume differences would yield the total specific free volume. The volume fractions of holes at different sizes were simply calcu-

Table 5. Measured Zero-pressure-weight-fraction Henry's Constants for the Hydrocarbons Used in HDPE and Five ss-EOs with Different Branch Contents at 170, 190, 210 and 230 °C Respectively

	polymer																							
	HDPE temperature (°C)				ss-EO-1 temperature (°C)				ss-EO-2 temperature (°C)				ss-EO-3 temperature (°C)				ss-EO-4 temperature (°C)				ss-EO-5 temperature (°C)			
solute	170	190	210	230	170	190	210	230	170	190	210	230	170	190	210	230	170	190	210	230	170	190	210	230
1-hexene	65.6	85.7	111	140	63.2	85.0	106	134	59.1	80.8	90.5	121	66.7	95.8	132	158	71.8	89.2	122	160	67.7	92	106	143
n-hexane	59.6	80.0	103	128	57.1	75.2	97.4	122	55.4	74.8	88.4	110	61.1	82.3	115	137	63.1	83.4	112	146	63.9	86.1	104	125
benzene	38.5	54.4	71.3	98.2	37.4	51.5	68.4	83.8	37.2	48.0	60.2	79.2	38.5	52.8	75.5	94.9	44.2	57.8	78.4	103	42.1	56.7	74.8	92.3
cyclohexane	34.4	46.7	64.0	91.2	33.2	46.5	61.3	77.8	33.7	44.5	55.9	70.4	33.9	49.0	67.9	88.0	38.6	50.9	68.2	90.5	36.9	50.1	65.4	82.6
n-heptane	30.1	43.6	61.8	80.0	29.8	41.4	57.5	74.7	29.0	41.1	52.4	71.0	30.6	42.1	60.7	83.2	35.2	46.3	63.2	82.6	32.2	45.3	60.2	77.6
toluene	18.7	26.5	36.8	49.1	18.2	25.7	34.3	48.6	18.2	25.4	35.2	48.6	18.3	26.0	37.9	50.5	22.0	29.9	41.5	56.1	20.2	29.0	37.6	51.8
1-octene	17.7	25.9	36.2	49.1	16.9	24.0	32.3	46.6	16.8	23.5	31.1	45.3	17.5	25.1	37.4	50.9	20.0	28.2	39.9	53.2	19.0	27.1	37.0	51.2
octane	16.1	23.6	33.1	45.4	15.7	22.7	30.3	44.3	15.5	22.2	31.4	41.5	15.7	22.8	33.7	46.1	18.4	25.8	36.5	50.7	17.3	25.3	33.4	46.2
xylenes	9.44	14.0	20.0	29.7	9.15	13.4	18.6	27.3	9.40	13.5	19.7	27.4	9.33	13.6	20.0	28.9	11.2	15.9	22.4	31.7	10.4	15.2	20.5	28.9
n-nonane	8.65	13.2	19.3	28.1	8.39	12.6	18.1	26.6	8.57	12.8	18.9	26.4	8.47	12.7	19.1	27.4	9.84	14.8	21.0	31.1	9.39	14.3	19.7	27.8
n-dodecane	1.44	2.44	3.92	6.31	1.40	2.33	3.21	5.92	1.43	2.32	3.67	5.93	1.41	2.35	3.74	6.25	1.63	2.78	4.26	7.06	1.55	2.64	4.03	6.35
n-pentadecane	0.26	0.48	0.83	1.45	0.25	0.46	0.77	1.37	0.26	0.46	0.76	1.34	0.25	0.47	0.81	1.43	0.30	0.55	0.91	1.61	0.28	0.52	0.85	1.50

Table 6. Measured Infinite-dilution-weight-fraction Activity Coefficients for the Hydrocarbons Used in HDPE and Five ss-EOs with Different Branch Contents at 170, 190, 210, and 230 °C, Respectively

	polymer																							
	HDPE temperature (°C)				ss-EO-1 temperature (°C)				ss-EO-2 temperature (°C)				ss-EO-3 temperature (°C)				ss-EO-4 temperature (°C)				ss-EO-5 temperature (°C)			
solute	170	190	210	230	170	190	210	230	170	190	210	230	170	190	210	230	170	190	210	230	170	190	210	230
1-hexene	1.95	1.95	1.98	2.05	1.92	1.96	1.97	2.08	1.88	1.98	1.89	2.08	1.91	2.00	2.08	2.11	2.04	2.01	2.11	2.26	1.99	2.04	1.97	2.15
n-hexane	1.95	1.97	1.98	2.03	1.91	1.92	1.97	2.05	1.91	1.98	1.95	2.04	1.92	1.95	2.04	2.03	2.01	2.03	2.11	2.23	2.02	2.06	2.03	2.07
benzene	1.66	1.70	1.69	1.77	1.63	1.65	1.67	1.65	1.64	1.62	1.59	1.65	1.63	1.64	1.71	1.69	1.80	1.77	1.81	1.84	1.75	1.75	1.76	1.75
cyclohexane	1.62	1.62	1.67	1.79	1.58	1.63	1.65	1.67	1.61	1.62	1.61	1.63	1.58	1.64	1.70	1.71	1.73	1.72	1.76	1.83	1.69	1.70	1.72	1.74
n-heptane	1.85	1.89	1.95	1.96	1.84	1.85	1.91	1.94	1.83	1.88	1.87	1.96	1.83	1.83	1.90	1.95	2.01	1.96	2.00	2.04	1.91	1.94	1.95	1.98
toluene	1.60	1.59	1.60	1.60	1.57	1.56	1.55	1.62	1.58	1.58	1.60	1.63	1.56	1.55	1.61	1.61	1.76	1.72	1.73	1.77	1.68	1.69	1.64	1.69
1-octene	1.80	1.81	1.83	1.84	1.74	1.72	1.70	1.78	1.76	1.75	1.73	1.85	1.76	1.74	1.79	1.80	1.91	1.88	1.90	1.90	1.86	1.84	1.82	1.87
octane	1.80	1.81	1.81	1.84	1.77	1.77	1.74	1.85	1.77	1.78	1.82	1.83	1.75	1.75	1.81	1.83	1.93	1.90	1.93	1.98	1.87	1.88	1.84	1.89
xylenes	1.55	1.54	1.53	1.60	1.52	1.49	1.47	1.54	1.55	1.52	1.55	1.57	1.53	1.50	1.52	1.57	1.72	1.67	1.66	1.57	1.64	1.62	1.56	1.57
n-nonane	1.75	1.76	1.76	1.80	1.72	1.71	1.71	1.77	1.75	1.74	1.78	1.80	1.72	1.70	1.74	1.76	1.88	1.87	1.86	1.93	1.84	1.84	1.79	1.82
n-dodecane	1.63	1.59	1.57	1.60	1.60	1.54	1.37	1.54	1.62	1.55	1.51	1.56	1.60	1.55	1.52	1.58	1.75	1.72	1.61	1.71	1.70	1.67	1.60	1.61
n-pentadecane	1.57	1.49	1.41	1.42	1.54	1.46	1.35	1.37	1.57	1.44	1.33	1.34	1.55	1.48	1.39	1.40	1.70	1.70	1.51	1.52	1.65	1.58	1.44	1.46

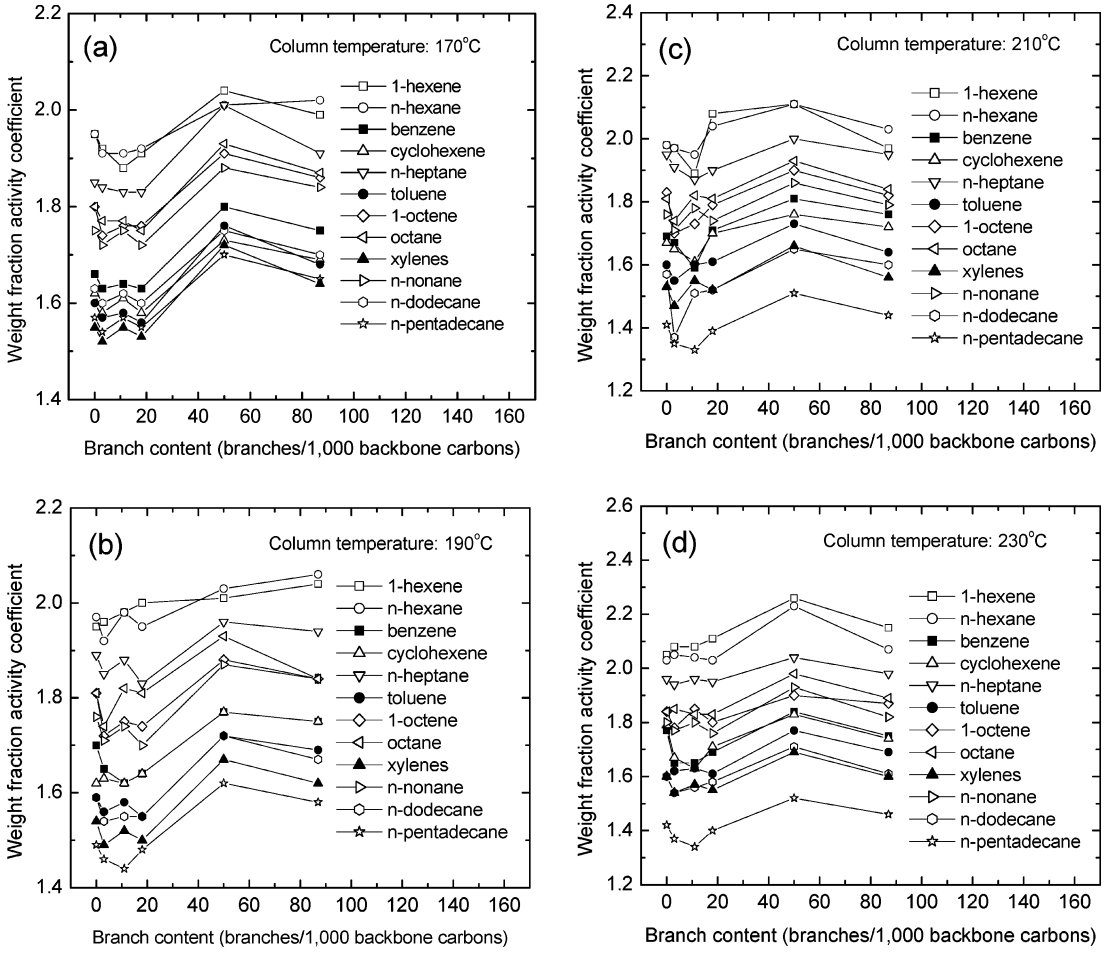

Figure 2. Branch content dependence of infinite-dilution-weight-fraction activity coefficient at four elevated temperatures (a) 170, (b) 190, (c) 210, and (d) 230 °C, respectively, for all 12 hydrocarbon solvents used.

lated by dividing the free volume of the holes at a specified size by the total specific free volume. It is obvious that the total specific free volume that we obtained in this manner did not include contributions from the free volume holes with radii that are smaller than 0.6 and larger than 3 Å. Since our main interest is in determining the effect of branch content on the size distribution of the free volume holes, we feel justified excluding those holes. In fact, as we will show in the next section, the total specific free volumes that we obtained for the polyethylene models are fairly close to the experimental values, indicating that contributions from the free volume holes outside the allowable size range of the probe to the total specific free volume are rather insignificant. The total and individual specific free volume values at various sizes for each model were computed by averaging the values of the last 100 picoseconds of the corresponding 1 ns trajectory.

Results and Discussion

All measured H_{12}^0 values are summarized in Table 5. Figure 1a−d shows the corresponding branch content dependence of H_{12}^0 for the 12 solvents used at 170, 190, 210, and 230 °C. It can be seen that, at 170 °C, H_{12}^0 values of the two solvents with the lowest normal boiling points (see Table 2) exhibited a minimum over the branch content range from 0 to 20, while all other solvents are more or less insensitive to the branch content of ss-EO. Such a feature becomes more pronounced for the low-boiling solvents and propagates to solvents with medium normal boiling points (100−150 °C) at higher experimental temperatures. Nonetheless, high boiling solvents (i.e., normal boiling points in the range of 150−300 °C) are not affected at all. Here, we use normal boiling points rather than vapor pressures of the solvents to signify the volatility of the solvents simply because experimental pressures were fairly close to the atmospheric pressure and experimental temperatures were well within the range of the normal boiling points of the solvents used. Because volatility of a solvent is an intrinsic property of the solvent and is independent of the molecular structure (i.e., branch content) of the polymer in the liquid phase, the observed H_{12}^0 behavior is clearly attributed to the interactions between the solvents and the polymers. Note that H_{12}^0 is controlled by the volatility of the solvent and the interaction between the solvent and the polymer.

To characterize solvent−polymer interactions, we measured their infinite-dilution-weight-fraction activity coefficients. Table 6 and Figure 2 summarize the results. It is clear that Ω_1^∞ varies more or less in a similar pattern to what we observed for H_{12}^0, confirming that it is mainly the interaction between the solvent and polymer that led to the observed branch content dependence of H_{12}^0. It can also be seen that solvents that exhibited a minimum in the H_{12}^0 versus branch content plots also did so in the Ω_1^∞ plots. However, Ω_1^∞ showed a slightly decreasing trend as a function of branch content

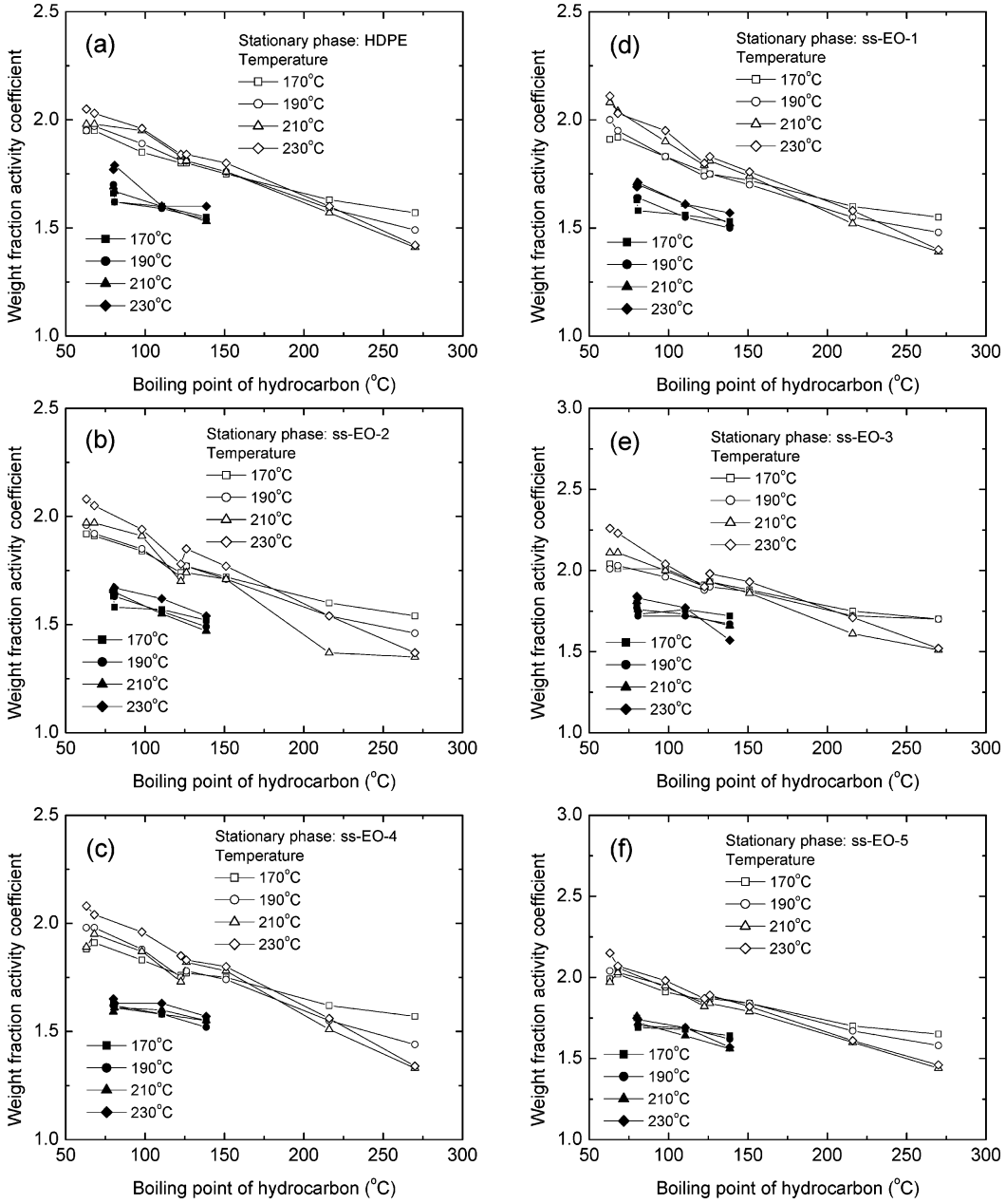

Figure 3. Plots of infinite-dilution-weight-fraction activity coefficients of the hydrocarbon solvents used in various ss-EOs vs their normal boiling points (a) HDPE, (b) ss-EO-1, (c) ss-EO-2, (d) ss-EO-3, (e) ss-EO-4, and (f) ss-EO-5, respectively, at temperatures of 170, 190, 210 and 230 °C.

in the high branch content region. Nonetheless, Ω_1^∞ values in the high branch content region are significantly higher than those in the lower branch content region for all the solvents used, but such differences become smaller at higher temperatures. The reason for which the branch content dependence of Ω_1^∞ does not manifest itself totally in the H_{12}^0 versus branch content plots, especially at low temperatures, for most of the solvents is simply because the experimental temperatures were only slightly higher or even below their normal boiling points. As a result, changes in the interactions between these solvents and the polymers are completely masked by the low volatility of the solvents. On the other hand, at 230 °C, Ω_1^∞ of most of the low- and medium-boiling solvents did not exhibit any noticeable minima, while such a feature still existed in the corresponding H_{12}^0 versus branch content plot. This is attributed to the fact that H_{12}^0 is much more sensitive to small changes in V_g^0 than in Ω_1^∞ (see eqs 3 and 4). At 230 °C, changes in V_g^0 are much smaller than those at lower temperatures for low- and medium-boiling solvents because the experimental temperature is much closer to their critical temperatures. What is required to explain in Figure 2 is the branch content dependence of Ω_1^∞.

It is well-known that the activity coefficient is a bulk thermodynamic quantity that signifies the degree of nonideality of a solution and the tendency of a particular substance to escape from the mixture in which other substances are present. The larger the activity coefficient of a substance is, the higher the tendency that the substance would leave the mixture. Data shown in Figure 2 simply suggests that, regardless of the volatility of the solvents, they all have a relatively higher tendency to escape from the high branch content ss-EOs (i.e., lower solubility) than the low branch content ones.

In the low branch content region (0−20) for certain solvents (mostly low- and medium-boiling solvents), they showed less tendency to escape from the ss-EO with a branch content of around 10, leading to the minima observed in the H_{12}^0 versus branch content plots. In general, solubility of one substance in another is mainly controlled by the degree of similarity between the intermolecular interactions (enthalpic in nature) and/or local packings of the molecules involved (entropic in nature). However, the data analysis shown below supports the idea that the observed branch content dependence of Ω_1^∞ is essentially an entropic-driven process.

First of all, if changes in Ω_1^∞ were a purely enthalpic-driven process, it would be expected that Ω_1^∞ should exhibit an inverse temperature dependence and that it should increase or decrease monotonically with increasing branch content of the polymer. For the temperature dependence, this is clearly not the case when the data shown in Figure 2 are replotted in Figure 3 when the normal boiling points of the solvents are used on the *x*-axis. Of particular interest in Figure 3 is that, for a given polymer, Ω_1^∞ values of both aliphatic and aromatic solvents decreased monotonically with increasing normal boiling point of the solvent with the aromatic series showing slightly lower Ω_1^∞ values than those of the aliphatic series. This trend, as one would expect for an enthalpic-driven process, is attributed mostly to the increasing intermolecular interaction strength between the solvent and the polymer rather than to the local packing effects. This is simply because it is unreasonable that larger solvent molecules would have a higher tendency to stay (a lower Ω_1^∞ value) in a polymer with constant free volume characteristics, as such molecules would possess relatively higher chemical potentials.[15] It should be noted that, in the extreme case, when there was no free volume in the polymer, no solvent, no matter how small it was and how favorably it would interact with the polymer, could exist in the bulk of the polymer ($\Omega_1^\infty = \infty$). Nonetheless, the normal boiling point (i.e., chemical structure) dependence of Ω_1^∞ for compounds with similar chemical structure shown in Figure 3 illustrates that a purely enthalpic-driven process should be dependent on structure in a monotonic fashion.

It seems that the observed branch content dependence of Ω_1^∞ is very likely attributed to the fitting of the sizes and geometry of the available free volume holes in the polymer and the solvent molecules. The present data suggest that low branch content ss-EOs would have local packing patterns that would yield free volume hole characteristics (e.g., average hole size and/or hole size distribution) that are suitable for the accommodation of more solvent molecules than that of the high branch content ss-EOs, leading to lower Ω_1^∞ values. The minima observed for certain solvents in the low branch content region may simply be due to the availability of a higher number of free volume holes with suitable sizes. It should be pointed out that the specific free volume of polyethylenes (i.e., total free volume per unit mass of the polymer) above the melting temperatures is essentially independent of their branching characteristics, as shown in Figure 4. Note that the specific free volumes shown in the figure were calculated on the basis of the pressure−volume−temperature data of Olabisi and Simha.[16] Therefore, the effect of branches is mainly on changing the free volume hole size distribution but not the specific free volume. In our view, such changes

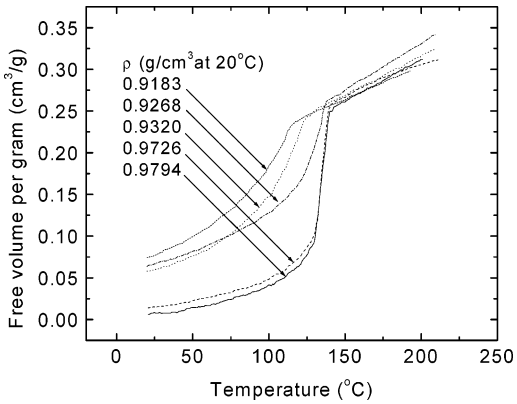

Figure 4. Calculated specific free volume of different types of polyethylenes at various temperatures on the basis of the pressure−volume−temperature data of Olabisi and Simha.[16]

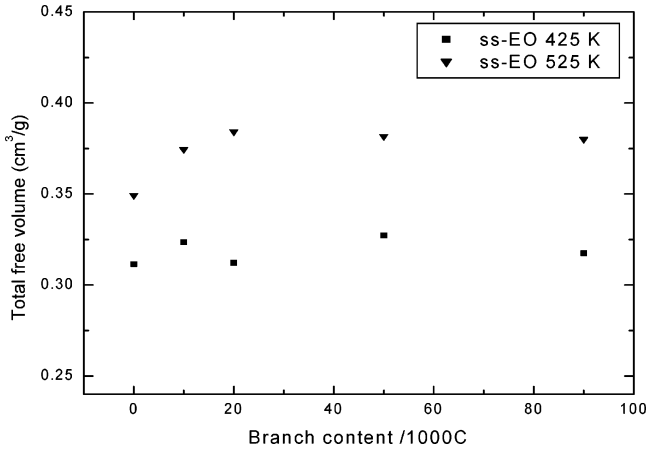

Figure 5. Branch content dependence of the specific free volume of the ss-EO models with branch contents ranging from 0 to 90 at 425 and 525 K.

would, in turn, alter the ability of ss-EO to absorb hydrocarbon solvents, leading to the observed branch content dependence of H_{12}^0 and Ω_1^∞. To verify our hypothesis, we carried out a series of MD simulations on model ss-EO molecules with branch contents ranging from 0 to 90 and calculated their free volume fractions of holes with different sizes at 425 and 525 K. Figures 5 and 6 depict such results.

The total free volumes per unit mass of the model systems calculated from MD simulations are shown in Figure 5. It is clear that both the branch content dependence of the specific free volume and the corresponding numerical values (0.32−0.37 cm^3/g from 152 to 252 °C) agree fairly well with experiment (0.28 to 0.36 cm^3/g from 150 to 250 °C obtained from Figure 4).[16] However, as speculated, the size distribution of the free volume holes changes considerably when branches are added to the backbone of ss-EO, regardless of the temperature (see Figure 6). In particular, at 425 K (Figure 6a and b), the volume fractions of holes with radii smaller than 1.5 Å increase slightly with increasing branch content, while those of the holes larger than 1.5 Å decrease with increasing branch content except for the models with branch contents of 10 and 20 at certain radii. Decrease in the volume fractions of the larger holes are consistent with our belief that branches generally reduce the number of holes (e.g., holes with radii of 0.6 and 3.0 Å correspond approximately to volumes of 0.9 and 113 $Å^3$, respectively) available for accommodating solvent molecules

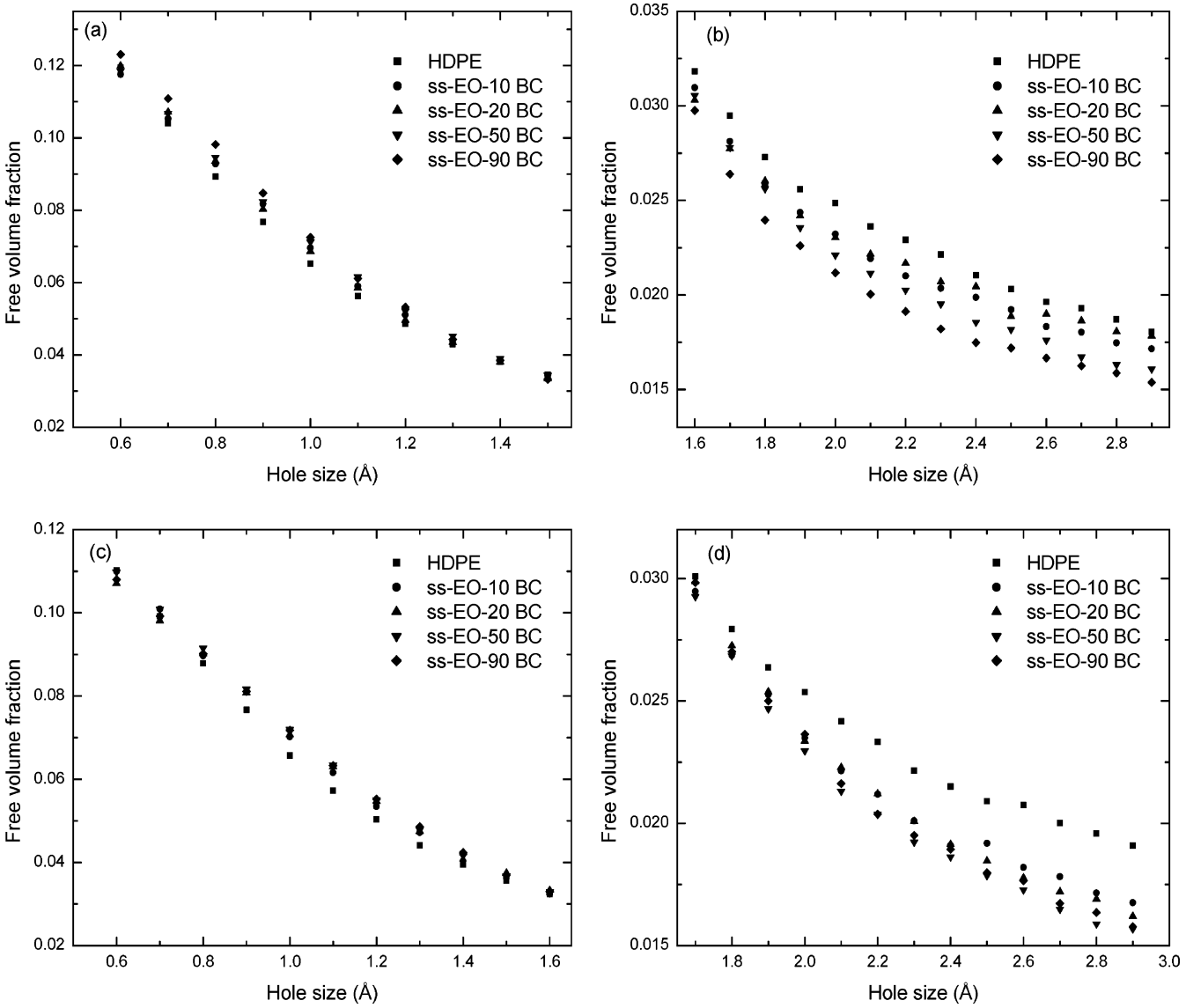

Figure 6. Computed free volume fractions using spherical probes with sizes ranging from 0.6 to 3.0 Å for the HDPE and ss-EO models described in the text at (a) 425 K, holes with sizes smaller than 1.5 Å, (b) 425 K, holes with sizes larger than 1.5 Å, (c) 525 K, holes with sizes smaller than 1.5 Å, and (d) 525 K, holes with sizes larger than 1.5 Å.

(see van der Waals volumes of the solvents shown in Table 2), leading to higher Ω_1^∞ values. It is worth noting that, in addition to size as quantified by spherical probes, geometry of free volume holes may also play a role here. However, since there exist no well-accepted methods for quantifying it, we chose to focus our discussion around the size of the free volume holes. Nonetheless, it seems that the observed minima in the H_{12}^0 and Ω_1^∞ versus branch content plots may be attributed to the nonmonotonic decreasing trend of the branch content dependence of the free volume fractions for the models with 10 and 20 branches. Figure 6c and d simply show that, except for HDPE, the branch content effect on the size distribution of the free volume holes becomes less pronounced at a higher temperature, which is consistent with our Ω_1^∞ results.

Conclusions

Two thermodynamic quantities, zero-pressure-weight-fraction Henry's constant (H_{12}^0) and infinite-dilution-weight-fraction activity coefficient (Ω_1^∞), were measured for 12 hydrocarbon solvents in a series of ethylene-1-octene copolymers (ss-EOs) with branch contents ranging from 0 to 87 branches per 1000 backbone carbons at four elevated temperatures using the technique of inverse gas chromatography. In general, low- and medium-boiling solvents exhibit a minimum in the branch content range of 0−20 when H_{12}^0 and Ω_1^∞ are plotted against the branch content of the polymer. However, over the branch content range of 20−87, both thermodynamic quantities are fairly insensitive to branch content. The observed branch content dependence of both H_{12}^0 and Ω_1^∞ were found to be attributed to the changes in the size distribution of the free volume holes rather than to differences in the intermolecular interaction characteristics. Molecular dynamics simulation results of comparable model ss-EO molecules with branch contents ranging from 0 to 90 support the above findings. In particular, the simulations showed that volume fraction of the free volume holes with radii larger than 1.5 Å decreased with increasing branch content except the models with 10 and 20 branches while the specific free volume stayed constant.

Acknowledgment. We thank NOVA Chemicals Corporation and the Natural Science Research Council of Canada for supporting this work financially. This research has been enabled by the use of WestGrid computing resources, which are funded in part by the Canada Foundation for Innovation, Alberta Innovation and Science, BC Advanced Education, and the participating research institutions. WestGrid equipment is provided by IBM, Hewlett-Packard, and SGI. P.C. would like to thank Wayne L. Mattice with whom he spent his sabbatical for calling attention to the study of the branch content dependence of H_{12}^0 over a wider range of branch contents of the ethylene-1-octene copolymer.

References and Notes

(1) Guichon, O.; Seguela, R.; David, L.; Vigier, G. *J. Polym. Sci., Part B: Polym. Phys.* **2003**, *41*, 327.
(2) Zhao, L.; Choi, P. *Macromol. Rapid Commun.* **2004**, *25*, 535.
(3) Prausnitz, J. M.; Lichtenthaler, R. N.; Gomes de Azevedo, E. *Molecular Thermodynamics of Fluid-Phase Equilibria*; 3rd ed.; Prentice Hall PTR: Upper Saddle River, 1999.
(4) Poling, B. E.; Prausnitz, J. M.; O′Connell, J. P. *The Properties of Gases and Liquids*; 5th ed.; McGraw-Hill Book Co.: New York, 2001.
(5) Zhao, Y. H.; Abraham, M. H.; Zissimos, A. M. *J. Org. Chem.*, **2003**, *68*, 7368.
(6) Lloyd, D. R.; Ward, T. C.; Schreiber H. P. *Inverse Gas Chromatography Characterization of Polymers and other Materials*; ACS Symposium Series 391; American Chemical Society: Washington, DC, 1989.
(7) Maloney D. P.; Prausnitz, J. M. *AIChE J.* **1976**, *22*, 74.
(8) DiPaola-Baranyi, G.; Guillet, J. E. *Macromolecules* **1978**, *11*, 228.
(9) Tsonopoulos, C. *AIChE J.* **1974**, *20*, 263.
(10) Mayo, S. L.; Olafson, B. D.; Goddard, W. A., III. *J. Phys. Chem.* **1990**, *94*, 8897.
(11) Choi, P. *Polymer* **2000**, *41*, 8741.
(12) Fan, Z. J.; Williams, M. C.; Choi, P. *Polymer* **2002**, *43*, 1497.
(13) Rudin, A.; Chee, K. K.; Shaw, J. H. *J. Polym. Sci., Part C* **1970**, *30*, 415.
(14) Nose, S. *J. Chem. Phys.* **1984**, *81*, 511.
(15) Xu, G.; Clancy, T. C.; Mattice, W. L.; Kumar S. K. *Macromolecules* **2002**, *35*, 3309.
(16) Olabisi O.; Simha, R. *Macromolecules* **1974**, *7*, 206.

MA0501904